

Cite this: *Analyst*, 2014, 139, 6580

One-step polymer screen-printing for microfluidic paper-based analytical device (μ PAD) fabrication†

 Yupaporn Sameenoi,^{*a} Piyaporn Na Nongkai,^a Souksanh Nouanthavong,^a
Charles S. Henry^b and Duangjai Nacapricha^c

We report a simple, low-cost, one-step fabrication method for microfluidic paper-based analytical devices (μ PAD) using only polystyrene and a patterned screen. The polystyrene solution applied through the screen penetrates through the paper, forming a three-dimensional hydrophobic barrier, defining a hydrophilic analysis zone. The optimal polystyrene concentration and paper types were first investigated. Adjusting polystyrene concentration allows for various types of paper to be used for successful device fabrication. Using an optimized polystyrene concentration with Whatman#4 filter paper, a linear relationship was found to exist between the design width and the printed width. The smallest hydrophilic channel and hydrophobic barrier that can be obtained are $670 \pm 50 \mu\text{m}$ and $380 \pm 40 \mu\text{m}$, respectively. High device-to-device fabrication reproducibility was achieved yielding a relative standard deviation (%RSD) in the range of 1.12–2.54% ($n = 64$) of the measured diameter of the well-shaped fabricated test zones with a designed diameter of 5 and 7 mm. To demonstrate the significance of the fabricated μ PAD, distance-based and well-based paper devices were constructed for the analysis of H_2O_2 and antioxidant activity, respectively. The analysis of H_2O_2 in real samples using distance-based measurement with CeO_2 nanoparticles as the colorimetric agent produced the same results at 95% confidence level, as those obtained using KMnO_4 titration. A proof-of-concept antioxidant activity determination based on the 2,2-diphenyl-1-picrylhydrazyl (DPPH) assay was also demonstrated. The results verify that the polymer screen-printing method can be used as an alternative method for μ PAD fabrication.

Received 2nd September 2014
Accepted 14th October 2014

DOI: 10.1039/c4an01624f

www.rsc.org/analyst

Introduction

Microfluidic paper-based analytical devices (μ PADs) are an attractive alternative for chemical analysis in several areas, including medical diagnostics,¹ clinical analysis,^{2–4} food testing⁵ and environmental monitoring,^{6–8} because they are inexpensive, portable, easy to use, biocompatible and can be easily disposed. μ PADs are obtained by patterning hydrophilic paper with impermeable barriers that define flow channels and test zones.^{9–11} The hydrophilic cellulose fiber network in the flow channel serves to be a self-priming capillary pump, allowing the wicking of solution without the need of external pumps. Unlike traditional analytical methods using cellulosic substrates, such as litmus paper, μ PADs are more efficient for complex chemical analysis, as well as more advanced sample pretreatment methods because of the ability to store reagents on the device.

Several methods have been demonstrated for μ PAD fabrication, including photolithography,¹² wax printing, screen printing and dipping,^{13–15} cutting,¹⁶ and inkjet etching.¹⁷ Photolithography was first reported for μ PAD fabrication using SU-8 photoresist and UV light for creating a hydrophobic barrier.¹⁸ This method is able to produce small channels (with a size as small as $750 \mu\text{m}$), in which the channel dimension can be controlled by the pattern of the UV mask.^{12,19} Photolithography, however, has some drawbacks, including expensive fabrication instrumentation (*e.g.*, spin coating and UV exposure system), complicated fabrication processes and solvent exposure to the hydrophilic region results in reduced paper flexibility and increased backgrounds for certain reactions.¹⁴ Wax printing has been the most widely used fabrication method because it is simple, rapid and uses common office equipment.^{13,20} Unfortunately, the method requires a relatively expensive printer and a heating step that causes wax spreading and decreases the feature resolution. Wax screen-printing is cheaper than wax printing because it requires only an inexpensive screen and a hotplate but also suffers from the loss of feature resolution as a result of wax spreading.¹⁴ Cutting by the use of an automated craft cutting machine provides a rapid and simple production of μ PADs without the need of organic solvents and/or heating.²¹ The major disadvantages of this

^aDepartment of Chemistry, Faculty of Science, Burapha University, Chon Buri, 20131, Thailand. E-mail: yupaporn@buu.ac.th; Fax: +66-38-393-494; Tel: +66-38-103-111

^bDepartment of Chemistry, Colorado State University, Fort Collins, 80523-1872, USA

^cDepartment of Chemistry and Center of Excellence for Innovation in Chemistry, Faculty of Science, Mahidol University, Bangkok, 10400, Thailand

† Electronic supplementary information (ESI) available. See DOI: 10.1039/c4an01624f

method include cost of the cutting machine and the inability to create small mechanically stable structures. Inkjet etching was performed by first dipping the paper into a polystyrene solution and then printing toluene multiple times using an inkjet printer.¹⁷ The toluene removed the polystyrene to create channels. Unfortunately, the printing step reduces channel reproducibility because it is difficult to align the paper ten consecutive times.

An ideal fabrication method for μ PADs would use inexpensive instrumentation and materials, allow a rapid fabrication for mass production, would be simple, and would not require the hydrophilic region to be exposed to solvent during fabrication. The technique should also provide high resolution and repeatability. Here, a polymer screen-printing method for μ PAD fabrication is reported that matches these requirements. The method uses a patterned screen and polystyrene dissolved in toluene for printing. The fabrication can be carried out in one step, where polystyrene solution is deposited onto the patterned screen placed over the paper. The polystyrene solution passes through the screen and paper in a single step. After the evaporation of solvent, a hydrophobic barrier remains, which provides high channel fidelity. The fabrication process is shown in Fig. 1. Polystyrene, a hydrophobic polymer, is inexpensive and easy to obtain. Similarly, screen-printing is a well-known and inexpensive method used worldwide for many printing processes. The new polymer screen-printing is performed in a single step without the requirement of external heat, UV light, clean room, printers, or complex instrumentation, making it ideal for inexpensive μ PAD fabrication in developing countries. The device is also flexible after fabrication, thus it can be used for complicated analysis that require bending and/or folding of the device. The mass production of μ PAD can be achieved using screening printing in a roll-to-roll format.

Here, the optimization of polystyrene concentration and paper types were first studied with the goal of providing well-defined hydrophobic barriers on the paper. Various types of paper can be fabricated using optimized polystyrene concentration. The resolution of the proposed fabrication method was evaluated and the smallest hydrophilic area and hydrophobic barrier that could be created were $670 \pm 50 \mu\text{m}$ and $380 \pm 40 \mu\text{m}$, respectively. We next studied the fabrication performance by comparing the screen pattern width with the width obtained on the paper; a linear relationship between the designed width

and the obtained width was found. The reproducibility of device-to-device fabrication was established in the range of 1.12–2.54% (relative standard deviation) for circular wells of 5 or 7 mm ($n = 64$). Finally, to demonstrate the analytical capability, we applied the fabrication method with CeO_2 nanoparticles as colorimetric probes to analyze H_2O_2 using an instrument-free distance-based detection method. The results showed no significant difference at 95% confidence level for the H_2O_2 analysis versus KMnO_4 titration. The fabrication μ PAD was also applied for the proof-of-concept analysis of antioxidant activity with the DPPH assay using gallic acid as a model antioxidant.

Experimental section

Reagents and materials

Whatman no. 1 and no. 4 filter papers were purchased from Whatman International Ltd (Maidstone, England). Kleenex® facial tissue was obtained from Kimberly Clark, Taiwan. Office paper was purchased from Kirin®, Thailand. Polystyrene was obtained from a stationery store in Chon Buri, Thailand. The patterned screen was obtained from local screen-printing shop (Chon Buri, Thailand). Toluene, H_2SO_4 , and methanol were all of analytical reagent grade and purchased from RCI Labscan Ltd (Bangkok, Thailand). Polyethylene glycol (PEG, MW 6000 g mol^{-1}), cerium(IV) oxide (CeO_2) nanoparticle (24.4% w/v) colloidal dispersion in 2.5% acetic acid with 10–20 nm particle sizes, DPPH and gallic acid were obtained from Sigma Aldrich (Saint Louis, Missouri, USA).

Fabrication of paper-based microfluidic devices

The device fabrication process is shown in Fig. 1. Screen patterns were generated using Adobe Illustrator. The screens were made from an 800 mesh polyester fabric on a wooden frame. To create a hydrophobic barrier, the patterned screen was placed onto a paper. The polystyrene solution, prepared by dissolving polystyrene in toluene, was applied over the screen. The polymer solution was squeezed to pass through the screen and penetrate to the bottom of the paper, creating a 3D patterned hydrophobic barrier. The patterned paper was ready to use after drying (<3 min by leaving in the hood and <1 min by fast drying by air-dryer). The screen was cleaned with toluene-

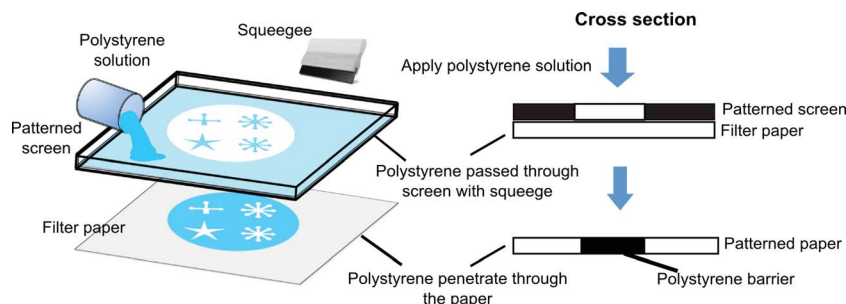


Fig. 1 Schematic of the one-step polymer screen-printing method for patterning hydrophobic barrier on the paper using polystyrene solution and a patterned screen.

soaked paper towel between subsequent device fabrications. All the steps were performed in a fume hood. Prior to running any assay, clear packing tape was added to the backside of the patterned paper to prevent leaking through the paper.

Distance-based detection of H₂O₂ using CeO₂ nanoparticles

The analysis of H₂O₂ was performed using the distance-based detection format. A thermometer-like patterned paper was fabricated using polymer screen-printing method.²² A circular shape of 6 mm diameter was created as a sample reservoir connected to a straight channel with a geometry of 3 mm wide and 8 cm long, which contained the reagents and served as the detection zone. CeO₂ nanoparticles were uniformly coated on the channel part of the patterned paper (detection zone, Fig. 6A) by dipping the paper in CeO₂ nanoparticle solution (3% w/v) and then allowing the paper to dry. The CeO₂ nanoparticles were hydrophobic, preventing wetting along the detection channel. To permit flow, the CeO₂ coated paper was dipped in polyethylene glycol solution (10 mg mL⁻¹ in deionized water), making the detection zone hydrophilic. 10 μL of H₂O₂ sample was pipetted onto the sample reservoir and allowed to flow along the detection channel. A rapid change from colorless to yellowish-orange of CeO₂ nanoparticles was observed on reaction with H₂O₂ because of the changes in their surface properties and chemical composition.^{23,24} Another 10 μL of deionized water was added to the sample reservoir to elute residual H₂O₂, which might remain in the sample zone (schematic diagram for the analytical procedure is shown in Fig. S-1a, ESI†). The distance developed by the color on the detection channel was directly proportional to the amount of H₂O₂ in the sample and was measured using a common ruler.

For method validation, a conventional KMnO₄ titration was used for H₂O₂ analysis.²⁵ Briefly, KMnO₄ used as a titrant was first standardized with acidified sodium oxalate solution. An aliquot of H₂O₂ samples was acidified with H₂SO₄ and titrated with KMnO₄ until the end-point was reached, where the color of KMnO₄ appeared.

Antioxidant activity analysis

To further evaluate the applicability of the fabricated μPAD, the paper was designed in a well-shaped format with a circular diameter of 5 mm. Antioxidant analysis was based on the DPPH assay using gallic acid as a model standard antioxidant.^{26,27} First, 1 μL of 1.5 mM DPPH in methanol was dropped onto the μPAD. Then, 1 μL gallic acid aqueous solutions at different concentrations were pipetted onto the well. The reaction proceeded for 15 min in the dark at room temperature (~27 °C) and the dried μPAD was obtained (schematic diagram for the analytical procedure is shown in Fig. S-1b, ESI†). The image of μPAD was obtained using a scanner and analyzed for violet color intensity using ImageJ (National Institute of Health, USA). The intensity measurement procedure is demonstrated in Fig. S-2 (ESI†).

Results and discussion

One-step fabrication of μPAD using polymer screen-printing

We present the use of inexpensive polystyrene as a printing material for the screen-printing of hydrophobic barriers onto filter paper for the fabrication of μPADs. The fabrication method involves one step (Fig. 1), in which the polymer solution passes through the patterned screen into the paper to form hydrophobic barriers. During the printing process, the toluene used as a solvent to dissolve polystyrene does not penetrate into the unpatterned areas because of the viscosity of the solution (Fig. S-3, ESI†). Polystyrene is widely available and very inexpensive. Furthermore, screen-printing is used for many applications ranging from clothing to electronics. Screens can be made from a variety of materials and can be produced in any country. Screen-printing has been used for the fabrication of biosensors and chemical sensors because it offers the advantages of low cost, mass production capabilities, and miniaturization.^{28–30}

We first evaluated the polystyrene concentration and paper types to determine the effect on spreading and penetration of the polystyrene into the paper. As shown in Fig. 2, both polystyrene concentration and paper type (Whatman #1, Whatman #4, facial tissue and office paper) impacted the structures of the final device. Higher polystyrene concentration results in a higher viscosity and reduction in the penetration of polystyrene into paper. Paper type also had a significant impact. For example, Whatman filter paper #4 (~20–25 μm) has larger pores than Whatman filter paper #1 (~11 μm) allowing the better penetration of the polystyrene solution. For Whatman filter paper #4 (Fig. 2, row 1), the lowest polystyrene concentration (20% w/v) provided the best penetration, but polystyrene spread into the paper was difficult to control, and it gave irreproducible dimensions. At the polystyrene concentrations of 30% (w/v), poor polystyrene penetration resulted in an incomplete three-dimensional hydrophobic barrier formation, as indicated by red ink spreading through the barriers. Using 25% w/v polystyrene with Whatman #4 well-defined patterns were obtained at the front and back of the paper. For Whatman #1, an incomplete hydrophobic barrier was observed on the paper at high polystyrene concentrations (15–20% w/v). At this viscosity with the small pore size of Whatman #1 (~11 μm), polystyrene could not penetrate through the paper. However, well-defined hydrophobic barrier on Whatman #1 paper could be formed using lower viscosity polystyrene solutions (10% w/v) because of the better penetration through the paper (Fig. 2, row 2). Previous studies have shown that polystyrene concentrations down to 5% have sufficient polystyrene to form a complete three-dimensional hydrophobic pattern on Whatman #1 paper.³¹ However, our results showed that a polystyrene concentration of less than 10% causes spreading of the polystyrene, with subsequent reduction in the reproducibility of the hydrophobic barrier dimensions (Fig. S-4, ESI†). We subsequently used facial and office paper as substrates (Fig. 2, row 3 and 4). Well-defined hydrophobic barriers were observed on these materials using the polystyrene concentrations of 10% and 20% (w/v). This

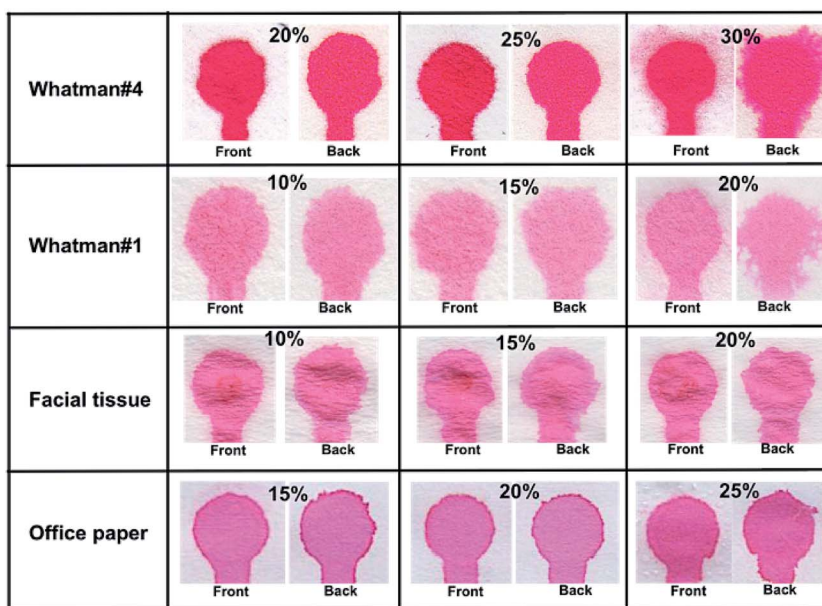


Fig. 2 Final patterned paper fabricated using polymer screen-printing method with the different concentrations of polystyrene in toluene (% w/v) and different types of paper. Red food dye was added to the polymer unfilled paper to indicate the hydrophilic region.

result demonstrates that the method is not limited to filter paper as a substrate. By adjusting the polymer concentration, complete hydrophobic barrier was obtained using the various types of paper. In comparison, the invented method offers a wider compatibility with several paper substrates than the instrument-dependent methods, such as flexographic printing,³¹ photolithography,¹² ink-jet printing,¹⁷ and wax-printing,¹³ where paper with low stiffness (*i.e.*, facial tissue) cannot be used due to the difficulty of feeding or aligning to the instrument during the fabrication process. In the subsequent studies, a polystyrene concentration of 25% w/v with Whatman #4 was used for μ PAD fabrication.

Various μ PAD patterns were constructed with well-defined hydrophobic barriers (Fig. 3). Pattern variations were made by adjusting the screen design, making the μ PAD suitable for both single-analyte (well format) and multi-analyte analysis (star-shaped format). In these images, clear borders were observed between the polymer filled and unfilled regions (Fig. 3a). The fabricated paper was further investigated using a microscope (Olympus, 20 \times magnification) (Fig. 3b); the investigation showed that the dye could not penetrate into the hydrophobic regions because of the polystyrene. Hydrophobicity of the paper was further confirmed by dropping the dye solution onto the polymer filled region and the intact paper. Dye rapidly wetted the hydrophilic paper region, but it was maintained as a drop on the hydrophobic region (Fig. 3c).

Resolution, reproducibility and stability

Pattern resolution was studied using the previously described methods.¹⁹ using the optimized fabrication parameters, the narrowest hydrophilic channel that the fabrication method could produce had a design width of 1000 μ m on the screen and a measured width of 671 ± 50 μ m ($n = 10$) on the fabricated

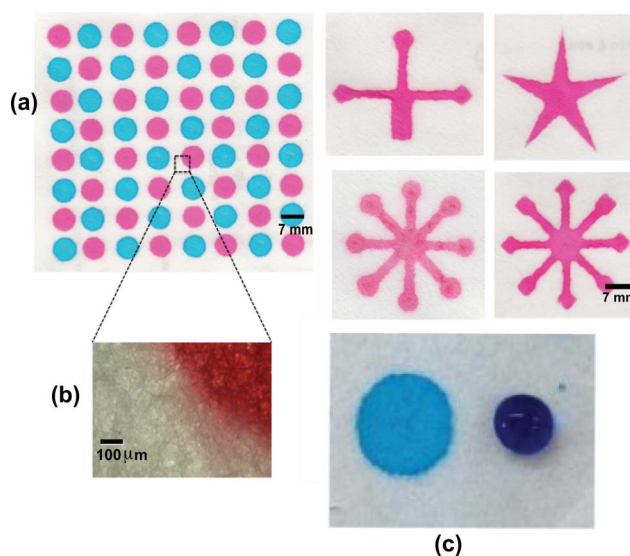


Fig. 3 Patterned paper fabricated using polymer screen-printing method: (a) representative patterns on the μ PADs with color in the hydrophilic zone and clear hydrophobic region, (b) hydrophobic-hydrophilic boundary imaged with a microscope (Olympus, 20 \times magnification), (c) a drop of dye solution (10 μ L) applied on the intact filter paper (well zones) and polymer coated region (the remaining part).

paper (Fig. 4a). The reduction in size relative to the screen size can be attributed to the spreading of the polystyrene into the paper. Higher concentrations, and therefore the higher viscosities of the polystyrene solution provide better resolution and a more accurate reproduction of the screen design. The resolution of hydrophobic barrier was also studied, where the narrowest designed barrier that could prevent the flow was 400 μ m,

which produced a measured width of $380 \pm 40 \mu\text{m}$ ($n = 10$) (Fig. 4b). Although finer details can be generated using photolithography,^{19,32} the dimensions obtained using the polymer screen-printing method are satisfactory for most of the μPAD applications.^{5–9,33} Fabrication performance was further evaluated by comparing the designed screen width and measured width. The results shown in Fig. 4c indicate that the resulting hydrophilic region corresponding to the designed width can be calculated using a linear equation, as follows: $W_a = 0.993W_d -$

420.7 ($R^2 = 0.992$), where W_a and W_d are actual width on the paper and the designed width on the screen, respectively.

The reproducibility of device-to-device fabrication was evaluated. Hydrophilic regions for 64 zones with a circular diameter of 5 and 7 mm were obtained (Fig. 5). The average diameter of the 64 microzones were 4.85 mm and 6.93 mm, which were in good agreement with the extrapolated values of ~ 4.54 mm and ~ 6.53 mm, calculated using the regression equation in Fig. 4c for designed widths of 5 mm and 7 mm, respectively. Relative standard deviations were 2.54% and 1.12%, respectively ($n = 64$), indicating the good fabrication reproducibility of the screen-printing method. Compared to other μPAD fabrication methods using polystyrene, our one-step printing method creates more reproducible μPAD structures than the inkjet etching and flexographic printing method (RSD of 3.8–11.7%).^{17,31,34} Our proposed method is also similar to or more reproducible than fabrication methods that use wax screen-printing and wax-dipping methods (RSD of 1.5–11.0%).^{14,15} Although, the reproducibility is similar, the polymer spreading is easier to control because it takes only one step for fabrication and no heating is required.

The fabricated μPAD was found to be very stable after more than 6 months storage because the hydrophobic barrier could prevent the leaking of the test solution similar to its initial ability. The patterned paper could be bent and folded without damaging the hydrophobic barrier, which makes it better than the μPADs fabricated using photolithography because they are rigid due to the SU-8 properties and could not be bent and folded.¹² The μPAD could also be immersed in some organic solvent several times without damaging the patterns because of the insolubility of the polystyrene in several solvents, such as methanol, ethanol, *n*-hexane and acetonitrile (Fig. S-5, ESI[†]). Therefore, the fabricated μPAD can be used for both complex chemical analysis, as well as cell-based assays that require multiple adding and rinsing steps in various solvents. This property makes the μPADs fabricated using polymer screen-printing superior to those obtained from a widely used wax printing method because wax materials cannot be used with any organic solvents because it is soluble in every organic solvent.⁹

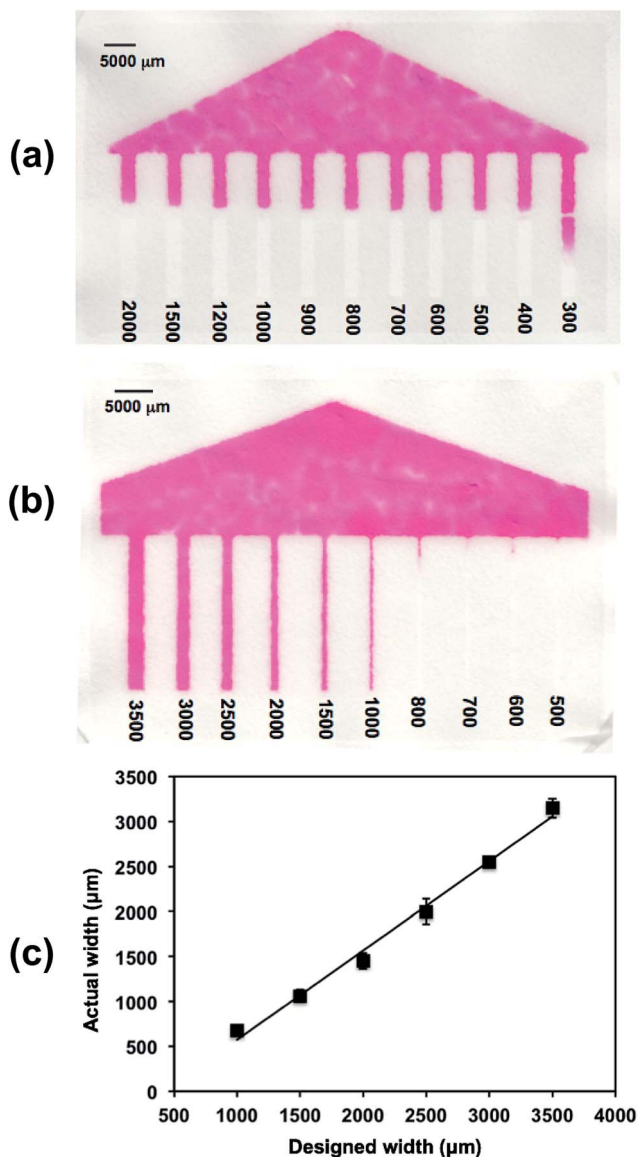


Fig. 4 Resolution study for the polymer screen-printing method. (a) The resolution of hydrophilic channel, where the smallest channel was $671 \pm 50 \mu\text{m}$ in size (1000 μm designed width). (b) The resolution of hydrophobic barrier, where the narrowest hydrophobic barrier that could prevent the flow of dye solution was $380 \pm 40 \mu\text{m}$ in size (400 μm designed width). (c) The quantitative comparison of the actual width of hydrophilic channels on the fabricated paper with the designed width on the patterned screen with the linear equation, $W_a = 0.993W_d - 420.7$ ($r^2 = 0.992$).

H_2O_2 analysis

The quantitative analysis of H_2O_2 is of significance because it is the product of many highly selective oxidase enzymes. H_2O_2 is also an important element in food, pharmaceutical, clinical and industrial products.^{35–37} Using the new fabrication method, a simple paper-based sensor combining distance-based detection with CeO_2 nanoparticles as colorimetric probes was constructed for H_2O_2 analysis. Henry's group recently introduced a distance-based measurement paper device, where quantification was achieved by measuring the length of a colored zone generated by the reaction of the analyte with an indicator along the hydrophilic channel.¹⁴ Here, CeO_2 nanoparticles were deposited along the channel labeled as detection zone (Fig. 6A). It was observed that CeO_2 nanoparticles endow certain hydrophobicity to the paper because of their hydrophobic properties at the surface.³⁸ When the solution was dropped on to CeO_2 -coated

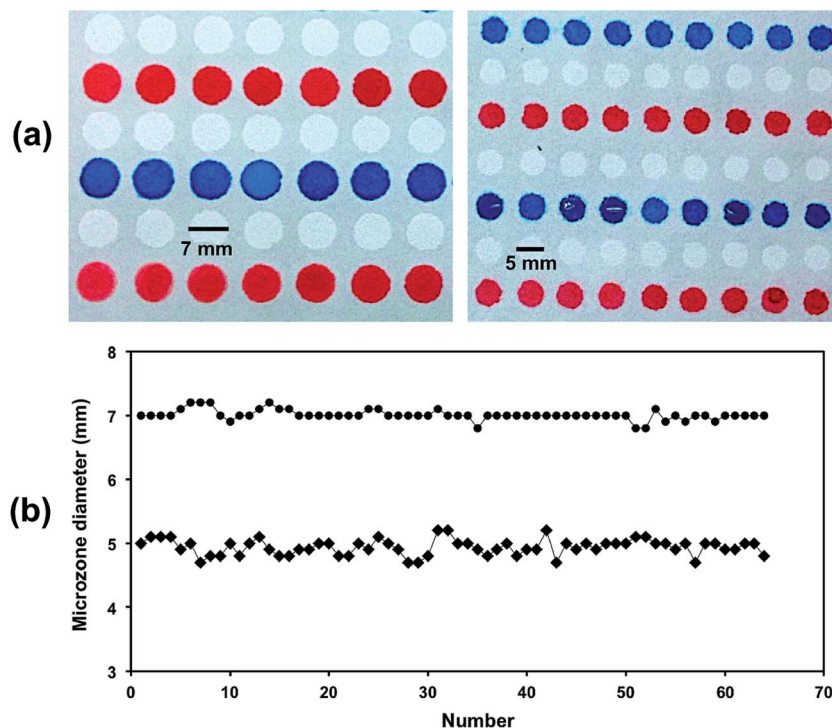


Fig. 5 (a) Arrays of paper-based microfluidic devices in well-shaped format with different circular diameters with blue and red ink on some hydrophilic regions. (b) The measured diameters of the 64 circular hydrophilic regions shown in part A, where the designed widths are 5 and 7 mm in diameters.

paper, only certain part of the solution could wick into the paper, and another portion appeared as a drop (Fig. S-6, ESI†). To enhance the hydrophobicity of the coated paper, a hydrophilic polymer, PEG, was added to increase the wicking of the analyte along the detection channel. H_2O_2 was then added to the sample zone and allowed to move through the channel, which reacted with CeO_2 nanoparticles to generate a yellowish-orange product. The studies have reported that CeO_2 nanoparticles consists of a mixture Ce^{3+} and Ce^{4+} oxidation states.²³ The addition of H_2O_2 induced the oxidation of Ce^{3+} to Ce^{4+} , resulting in changes to $\text{Ce}^{3+}/\text{Ce}^{4+}$ ratio causing the resulting color (list of the chemical equations is shown in ESI†).²⁴ The results of H_2O_2 analysis are shown in Fig. 6. A longer yellowish-orange distance was observed with higher H_2O_2 concentration. A linear calibration curve was constructed by plotting the resulting distances as a function of H_2O_2 concentration for quantitative analysis ($Y = 0.0698X + 13.928$, $R^2 = 0.990$, %RSD of three different H_2O_2 concentration in the linear range $<15.3\%$ ($n = 5$). Use of the μPADs was demonstrated using three commercially available samples, including one hair bleaching agent (6% H_2O_2) and two topical anti-infective solutions (3% H_2O_2). For μPAD analysis, all the samples were diluted to approximate concentrations that fall in the linear range of assay. Table 1 compares H_2O_2 measured using the μPAD analysis to the concentrations measured using KMnO_4 titration.²⁵ Using the paired t -test, no statistical differences were observed at 95% confidence level between the μPAD method and KMnO_4 titration (two-tailed $P = 0.6257$). Moreover, comparison between the μPAD method and label values showed that there is no significant difference at 95% confidence level (two-tailed $P =$

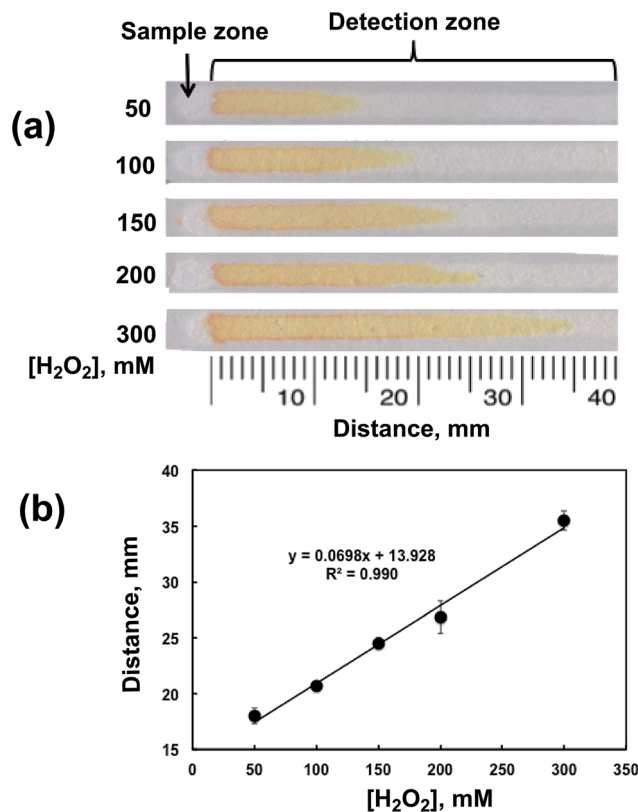


Fig. 6 Distance-based measurement μPAD for H_2O_2 analysis using CeO_2 nanoparticles as a colorimetric reagent. (a) μPAD image after the analysis of different H_2O_2 concentrations. (b) Linear calibration curve plotted measuring distance of the apparent color as a function of H_2O_2 concentrations.

Table 1 Determination of H₂O₂ in real samples

Samples	H ₂ O ₂ (% w/w) (<i>n</i> = 3)		
	Labeled value	KMnO ₄ titration	Distance-based μ PAD
Hair bleach	6	6.53 \pm 0.02	6.68 \pm 0.22
Anti-infective 1	3	3.40 \pm 0.06	3.37 \pm 0.06
Anti-infective 2	3	3.03 \pm 0.10	3.08 \pm 0.16

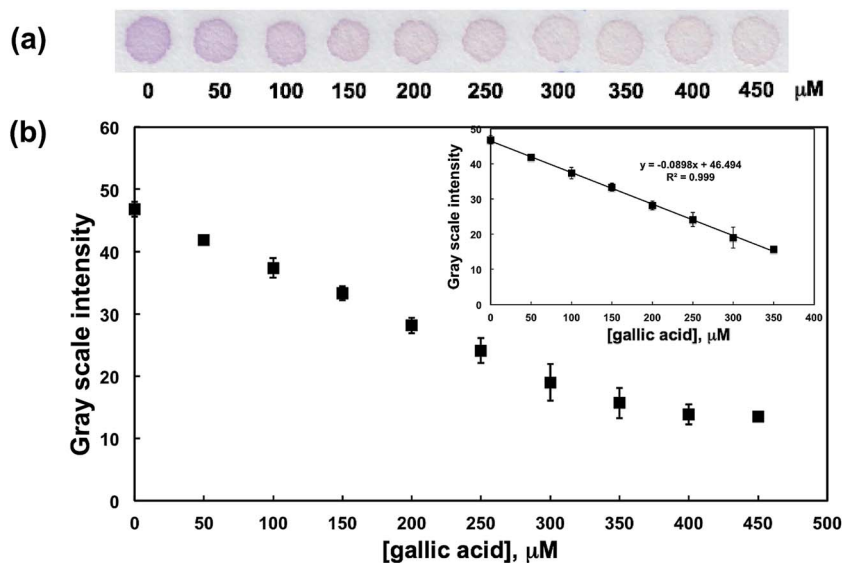


Fig. 7 Analysis of antioxidant activity based on DPPH assay using the fabricated μ PADs in a well-shaped format. (a) Image of paper devices consisting of multiple 5 mm wells for the analysis of gallic acid with standard antioxidant at 0–450 μ M. (b) Dose–response curve plotting gray scale intensity converted from violet color versus the concentrations of gallic acid (*n* = 3) and inset is the linear portion of the curve.

0.1617). Both the results demonstrate the viability of the method for H₂O₂ analysis in real samples.

Antioxidant activity

To further evaluate the applicability of the fabrication method, the analysis of antioxidant activity using DPPH assay was studied. Attention on antioxidants has been growing because of their suggested ability to inhibit cancer, support health and prevent several diseases, including heart disease, aging, and neurodegenerative diseases, such as Parkinson's and Alzheimer's disease.^{39,40} The epidemiological studies have shown a link between the decrease of aforementioned diseases and the consumption of food that are rich in antioxidants, including fruits, wines, herbs and vegetables.^{40,41} Because of this encouragement, there has been a growing interest in the development of analytical methods to assess the antioxidant activity of foods. In this work, as a proof-of-concept for antioxidant activity analysis, well-shaped detection zones of 5 mm diameter were fabricated for the analysis of gallic acid, as a model antioxidant using the DPPH assay. The design facilitated the quantitative analysis of antioxidant by determining the changes in DPPH color intensity upon the addition of antioxidant using imaging software. When reacted with antioxidants, violet coloured free-radical DPPH is reduced, producing yellow stable DPPH

compounds. The chemical reaction of DPPH and antioxidant is shown in Fig. S-7 (ESI[†]). The decrease in the intensity of violet color is directly proportional to the antioxidant activity. The results of a proof-of-concept determination of antioxidant activity using gallic acid as a model standard antioxidant are shown in Fig. 7. The intensity of violet colour of free-radical DPPH decreased as gallic acid concentrations increased from 0 to 450 μ M (Fig. 7a). A dose–response curve was constructed by plotting gray scale intensity as a function of gallic acid concentration. The dynamic linear range was in the range of 0–350 μ M gallic acid; the relative standard deviation was in the range of 4.66–9.61% (*n* = 5). The detection limit for gallic acid was 33.3 μ M. These analytical features were similar to those obtained from the traditional DPPH assay, indicating that the DPPH- μ PAD assay is promising for antioxidant analysis.^{42,43} The μ PAD assay can be performed in high throughput mode, where more than 20 samples can be quantified in 15 min. The assay also works with samples in the range of microliters, which is thousand fold less than the traditional DPPH assay.^{44,45}

Conclusion

We have demonstrated the use of one-step polymer screen-printing to be a simple, low-cost and rapid method for the

fabrication of μ PAD. Under the optimal condition, the method provides well-defined hydrophobic barrier with an efficient resolution and high reproducibility without the need of complicated and expensive instruments. Various μ PAD formats can be created by adjusting the screen pattern. An efficient resolution was achieved, where the smallest hydrophilic channel and hydrophobic barrier are $671 \pm 50 \mu\text{m}$ and $380 \pm 40 \mu\text{m}$, respectively. Highly reproducible fabrication was obtained from 64 devices with %RSD in the range of 1.12–2.54%. The application of the fabricated μ PAD for the chemical analysis of real world samples was successfully demonstrated. The μ PAD with distance-based detection was used to determine H_2O_2 amount in real samples using CeO_2 nanoparticles as colorimetric probes. No significant difference was found at 95% confidence level between the H_2O_2 amount obtained from the μ PAD and those from the conventional method. The μ PAD was further demonstrated for its ability to measure antioxidant activity analysis based on DPPH assay. These demonstrations indicated that the polymer screen-printing method is an alternative method for μ PAD fabrication, which is suitable for developing countries, and amenable to further modification for complex chemical analysis, bio-analysis and cell-based study.

Acknowledgements

This work was supported by DPST Research Grant 013/2557 from the Institute for the Promotion of Teaching Science and Technology, Thailand and the grant from the Higher Education Research Promotion and National Research University Project of Thailand, Office of the Higher Education Commission, Thailand.

References

- 1 S. J. Vella, P. Beattie, R. Cademartiri, A. Laromaine, A. W. Martinez, S. T. Phillips, K. A. Mirica and G. M. Whitesides, *Anal. Chem.*, 2012, **84**, 2883.
- 2 J. Yu, L. Ge, J. Huang, S. Wang and S. Ge, *Lab Chip*, 2011, **11**, 1286.
- 3 W. Dungchai, O. Chailapakul and C. S. Henry, *Anal. Chem.*, 2009, **81**, 5821.
- 4 W. Dungchai, O. Chailapakul and C. S. Henry, *Anal. Chim. Acta*, 2010, **674**, 227.
- 5 J. C. Jokerst, J. A. Adkins, B. Bisha, M. M. Mentele, L. D. Goodridge and C. S. Henry, *Anal. Chem.*, 2012, **84**, 2900.
- 6 Y. Sameenoi, P. Panyameesamer, N. Supalakorn, K. Koehler, O. Chailapakul, C. S. Henry and J. Volckens, *Environ. Sci. Technol.*, 2012, **47**, 932.
- 7 M. M. Mentele, J. Cunningham, K. Koehler, J. Volckens and C. S. Henry, *Anal. Chem.*, 2012, **84**, 4474.
- 8 W. Dungchai, Y. Sameenoi, O. Chailapakul, J. Volckens and C. S. Henry, *Analyst*, 2013, **138**, 6766.
- 9 A. K. Yetisen, M. S. Akram and C. R. Lowe, *Lab Chip*, 2013, **13**, 2210.
- 10 J. Hu, S. Wang, L. Wang, F. Li, B. Pinguang-Murphy, T. J. Lu and F. Xu, *Biosens. Bioelectron.*, 2014, **54**, 585.
- 11 X. Li, D. R. Ballerini and W. Shen, *Biomicrofluidics*, 2012, **6**, 011301.
- 12 A. W. Martinez, S. T. Phillips, E. Carrilho, S. W. Thomas III, H. Sindi and G. M. Whitesides, *Anal. Chem.*, 2008, **80**, 3699.
- 13 E. Carrilho, A. W. Martinez and G. M. Whitesides, *Anal. Chem.*, 2009, **81**, 7091.
- 14 W. Dungchai, O. Chailapakul and C. S. Henry, *Analyst*, 2011, **136**, 77.
- 15 T. Songjaroen, W. Dungchai, O. Chailapakul and W. Laiwattanapaisal, *Talanta*, 2011, **85**, 2587.
- 16 D. A. Bartholomeusz, R. W. Boulté and J. D. Andrade, *J. Microelectromech. Syst.*, 2005, **14**, 1364.
- 17 K. Abe, K. Suzuki and D. Citterio, *Anal. Chem.*, 2008, **80**, 6928.
- 18 A. W. Martinez, S. T. Phillips, M. J. Butte and G. M. Whitesides, *Angew. Chem., Int. Ed.*, 2007, **46**, 1318.
- 19 A. W. Martinez, S. T. Phillips, B. J. Wiley, M. Gupta and G. M. Whitesides, *Lab Chip*, 2008, **8**, 2146.
- 20 Y. Lu, W. Shi, L. Jiang, J. Qin and B. Lin, *Electrophoresis*, 2009, **30**, 1497.
- 21 E. M. Fenton, M. R. Mascarenas, G. P. López and S. S. Sibbett, *ACS Appl. Mater. Interfaces*, 2008, **1**, 124.
- 22 D. M. Cate, W. Dungchai, J. C. Cunningham, J. Volckens and C. S. Henry, *Lab Chip*, 2013, **13**, 2397.
- 23 J. D. Gaynor, A. S. Karakoti, T. Inerbaev, S. Sanghavi, P. Nachimuthu, V. Shutthanandan, S. Seal and S. Thevuthasan, *J. Mater. Chem. B*, 2013, **1**, 3443.
- 24 M. Ornatska, E. Sharpe, D. Andreescu and S. Andreescu, *Anal. Chem.*, 2011, **83**, 4273.
- 25 N. V. Klassen, D. Marchington and H. C. E. McGowan, *Anal. Chem.*, 1994, **66**, 2921.
- 26 M. K. Roy, M. Koide, T. P. Rao, T. Okubo, Y. Ogasawara and L. R. Juneja, *Int. J. Food Sci. Nutr.*, 2010, **61**, 109.
- 27 K. Schlesier, M. Harwat, V. Böhm and R. Bitsch, *Free Radical Res.*, 2002, **36**, 177.
- 28 M. Tudorache and C. Bala, *Anal. Bioanal. Chem.*, 2007, **388**, 565.
- 29 J. Wang, *Chem. Rev.*, 2008, **108**, 814.
- 30 J. P. Metters, R. O. Kadara and C. E. Banks, *Analyst*, 2011, **136**, 1067.
- 31 J. Olkkonen, K. Lehtinen and T. Erho, *Anal. Chem.*, 2010, **82**, 10246.
- 32 Q. He, C. Ma, X. Hu and H. Chen, *Anal. Chem.*, 2013, **85**, 1327.
- 33 X. Mu, L. Zhang, S. Chang, W. Cui and Z. Zheng, *Anal. Chem.*, 2014, **86**, 5338.
- 34 K. Abe, K. Kotera, K. Suzuki and D. Citterio, *Anal. Bioanal. Chem.*, 2010, **398**, 885.
- 35 S.-Q. Liu and H.-X. Ju, *Anal. Biochem.*, 2002, **307**, 110.
- 36 Y. Xiao, H.-X. Ju and H.-Y. Chen, *Anal. Chim. Acta*, 1999, **391**, 73.
- 37 T. You, O. Niwa, M. Tomita and S. Hirono, *Anal. Chem.*, 2003, **75**, 2080.
- 38 G. Azimi, R. Dhiman, H.-M. Kwon, A. T. Paxson and K. K. Varanasi, *Nat. Mater.*, 2013, **12**, 315.
- 39 L. H. Yao, Y. Jiang, J. Shi, F. Tomas-Barberan, N. Datta, R. Singanusong and S. Chen, *Plant Foods Hum. Nutr.*, 2004, **59**, 113.

- 40 C. Kaur and H. C. Kapoor, *Int. J. Food Sci. Technol.*, 2001, **36**, 703.
- 41 J. Sun, Y.-F. Chu, X. Wu and R. H. Liu, *J. Agric. Food Chem.*, 2002, **50**, 7449.
- 42 E. V. Piletska, S. S. Piletsky, M. J. Whitcombe, I. Chianella and S. A. Piletsky, *Anal. Chem.*, 2012, **84**, 2038.
- 43 Z. Cheng, J. Moore and L. Yu, *J. Agric. Food Chem.*, 2006, **54**, 7429.
- 44 C. Sánchez-Moreno, J. A. Larrauri and F. Saura-Calixto, *J. Sci. Food Agric.*, 1998, **76**, 270.
- 45 M. Ozgen, R. N. Reese, A. Z. Tulio, J. C. Scheerens and A. R. Miller, *J. Agric. Food Chem.*, 2006, **54**, 1151.